Physica B 404 (2009) 2263–2269

Contents lists available at ScienceDirect

Physica B

journal homepage: www.elsevier.com/locate/physb

A kinetic study of non-isothermal decomposition process of anhydrous nickel nitrate under air atmosphere

B. Janković [a,*], S. Mentus [a], D. Jelić [b]

[a] Faculty of Physical Chemistry, University of Belgrade, Studentski Trg 12-16, P. O. Box 137, 11001 Belgrade, Serbia
[b] Faculty of Medicine, University of Banja Luka, 78000 Banja Luka, Bosnia and Herzegovina

ARTICLE INFO

Article history:
Received 1 April 2009
Accepted 17 April 2009

Keywords:
Kinetics
Non-isothermal decomposition
Thermogravimetric analysis
Surface properties

ABSTRACT

The non-isothermal decomposition process of anhydrous nickel nitrate under air atmosphere was investigated. The kinetic analysis of decomposition process was performed using Friedman (FR), Kissinger–Akahira–Sunose (KAS) and Flynn–Wall–Ozawa (FWO) isoconversional methods. The kinetic model was determined by the Málek's method. The composite differential method I was used for checking the established reaction model. It was found that the value of E_a calculated by composite differential method ($E_a = 147.1\ \mathrm{kJ\,mol^{-1}}$) represents the medium value between the values of the apparent activation energy calculated by FR ($E_{a,FR} = 152.8\ \mathrm{kJ\,mol^{-1}}$) and FWO ($E_{a,FWO} = 143.1\ \mathrm{kJ\,mol^{-1}}$) methods. Using two special functions ($y(\alpha)$ and $z(\alpha)$), it was found that the two-parameter autocatalytic model (Šesták–Berggren (SB) kinetic model) with kinetic exponents $M = 0.23$ and $N = 1.14$ is the most adequate one to describe the decomposition kinetics of the studied system at various heating rates. The obtained non-isothermal differential conversion curves from the experimental data show the results being accordant with those theoretically calculated. It was concluded that the SB kinetic model can be used for a quantitative description of non-isothermal decomposition process of anhydrous nickel nitrate which involves the partially overlapping nucleation and growth phases.

1. Introduction

Nickel compounds and metallic nickel have many industrial and commercial applications including use in stainless steels and other nickel alloys, catalysts, batteries, pigments, and ceramics. Nickel salts are green to yellow crystals that generally are soluble in water and decompose when heated. Nickel nitrates are commercially available in anhydrous $-Ni(NO_3)_2$, and hydrous $-Ni(NO_3)_2 \cdot 6H_2O$ forms. The main use of nickel nitrate is in the production of catalysts, especially sulfur sensitive catalysts, and as an intermediate in the production of nickel–cadmium batteries. Nickel nitrate is also used to make products used in the pretreatment of metals prior to painting and prior to cold-forming processes. Like other nitrates, nickel nitrate is oxidizing, so that caution should be exercised when it contacts with reducing materials such as organic substances. Nickel nitrate is a suspected carcinogen, along with the most other nickel compounds [1,2].

Nickel nitrate may be synthesized by the leaching of nickel metal (e.g. broken cathodes, briquettes, nickel sheets) in nitric acid solution [3,4]. Solid nickel nitrate can be produced by concentrating this solution [3,4].

Thermal decomposition of nickel nitrate hexahydrate has been widely studied [5–8], and under controlled water pressure, anhydrous nickel nitrate may be obtained, being the direct precursor of NiO.

The decomposition of anhydrous nickel nitrate was studied under different experimental conditions by the various researchers [9–14]. Criado et al. [9,10] investigated the thermal decomposition of anhydrous nickel nitrate by the isothermal and non-isothermal thermogravimetry, using "in situ" drying of hexahydrate (at $T = 150\ ^\circ\mathrm{C}$) to obtain anhydrous salt. These authors claimed that the decomposition process follows the Avrami–Erofeev law with the kinetic exponent $n = 2$ and with the activation energy close to $84\ \mathrm{kJ\,mol^{-1}}$ [9]. They found that the investigated decomposition process occurs in a single-step mechanism. In addition, this process was usually used as 'example reaction' for checking some new methods for the kinetic analysis of solid state reactions [10–13]. After a detailed literature survey, we have not found that the conclusions on the decomposition of anhydrous nickel nitrate [9–11] were reconsidered anywhere.

In this study, the decomposition of anhydrous nickel nitrate was observed by thermogravimetry under linearly programmed heating, and the obtained results were analyzed from the kinetically point of view. The aim of the kinetic analysis is determination of kinetic triplet (i.e. kinetic model (reaction mechanism), $f(\alpha)$, the apparent activation energy, E_a, and the

* Corresponding author. Tel./fax: +381 11 2187 133.
E-mail address: bojanjan@ffh.bg.ac.rs (B. Janković).

0921-4526/$ - see front matter © 2009 Elsevier B.V. All rights reserved.
doi:10.1016/j.physb.2009.04.024

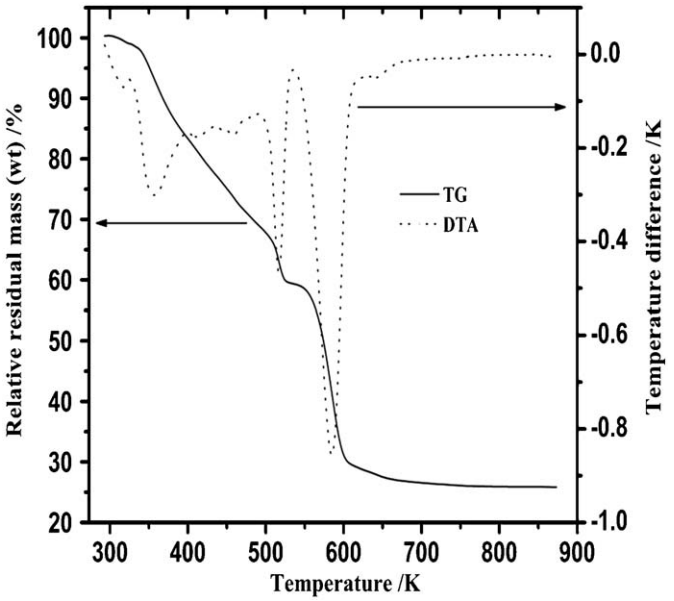

Fig. 1. Simultaneously recorded TG and DTA curves for the non-isothermal decomposition of Ni(NO3)2 · 6H2O at heating rate of 15 K min^{-1} in air atmosphere at a rate of 90 mL min^{-1}.

pre-exponential factor, A) for the investigated decomposition process.

2. Experimental

2.1. Materials and methods

Thermal decomposition of $Ni(NO_3)_2 \cdot 6H_2O$ (Merck, 99.5%) was studied by thermogravimetry using a TA SDT 2960 thermobalance, enabling simultaneous recording of TGA and DTA curves. Purging gas was air, at a flowing rate of $\varphi = 90\,mL\,min^{-1}$. The furnace temperature rose linearly at heating rates: $\beta = 5$, 15 and 30 K min^{-1}, in the temperature range from an ambient one up to 875 K.

Criado et al. [9,10] produced anhydrous nickel nitrate "in situ", i.e. within the thermobalance, by the isothermal heating of the hexahydrate at 150 °C (423 K), before to subject them to thermal decomposition. In this study, upon recording complete TG curve of hexahydrate decomposition (Fig. 1), we perceived that dehydration of hexahydrate finishes completely before the anhydrous salt commences to decompose: namely a clearly distinct plateau belonging to anhydrous salt is visible at nearly 525 K. Thus, we recorded thermograms of nickel nitrate haxahydrate at three different heating rates, and underwent to kinetic analysis that part of TG curves pertaining to the decomposition of anhydrous salt. Consequently, we applied in this study a technique of non-isothermal "in situ" dehydration of nickel nitrate hexahydrate, in order to study the kinetics of anhydrous salt decomposition.

3. Theoretical background

For the non-isothermal experimental conditions, the reaction rate can be expressed as

$$\beta \frac{d\alpha}{dT} = A \exp\left(-\frac{E_a}{RT}\right) f(\alpha) \tag{1}$$

where β stands for the experiment heating rate, A is the pre-exponential (frequency) factor (which gives an idea of the association tendency of reacting molecules), E_a is the apparent activation energy, T is the absolute temperature, R is the universal gas constant, and $f(\alpha)$ is the unknown function of conversion (non-isothermally, the conversion fraction (α) at any temperature is $\alpha = (m_0 - m_T)/(m_0 - m_f)$ where m_0, m_T and m_f represents the initial, actual and final mass of the investigated sample, respectively).

From Eq. (1), taking logarithms:

$$\ln\left[\beta_i\left(\frac{d\alpha}{dT}\right)\right] = \ln[Af(\alpha)] - \frac{E_a}{RT_\alpha} \tag{2}$$

where T_α is the temperature at which the system approach a conversion α, and β_i is a determined heating rate. For a constant α, a plot of $\ln[\beta_i(d\alpha/dT)]$ versus $1/T_\alpha$ should be a straight line whose slope allows the calculation of the apparent activation energy. Eq. (2) represents the main equation for the differential Friedman (FR) isoconversional method [15].

Integrating the differential non-isothermal rate law (Eq. (1)) produces the integral form of the non-isothermal rate law:

$$g(\alpha) = \frac{A}{\beta}\int_0^T \exp\left(-\frac{E_a}{RT}\right) dT \tag{3}$$

where $g(\alpha)$ is the integral function of conversion. The integral in Eq. (3) is called the "temperature integral" and has no analytic solution [16,17].

To transform the above integral to a more general form found in mathematical handbooks, the integration variable can be redefined as $x = E_a/RT$, and the temperature integral then becomes

$$g(\alpha) = \frac{AE_a}{\beta R}\int_x^\infty \frac{\exp(-x)}{x^2} dx \tag{4}$$

If

$$p(x) = \int_x^\infty \frac{\exp(-x)}{x^2} dx \tag{5}$$

then Eq. (4) can be written as

$$g(\alpha) = \frac{AE_a}{\beta R} p(x) \tag{6}$$

where $p(x)$ is the exponential integral which can be found in mathematical tables [18]. The main approaches used for evaluating the temperature/exponential integral are [16]: (a) calculating values of $p(x)$ numerically, (b) converting $p(x)$ to an approximate form that can be integrated and (c) approximating $p(x)$ by a series expansion.

Actually, integral isoconversional methods differ depending on the approximation of this integral. One of them is that given by Flynn and Wall [19], and Ozawa [20], which relies on Doyle approximation [21]:

$$\ln p(x) \approx -5.331 - 1.052x \tag{7}$$

Taking logarithms in Eq. (6) and substituting in Eq. (7), the following equation is valid:

$$\ln \beta = \ln\left[\frac{AE_a}{Rg(\alpha)}\right] - 5.331 - 1.052\frac{E_a}{RT} \tag{8}$$

For a constant conversion, a plot of $\ln\beta$ versus $1/T$, from the data at different heating rates, leads to a straight line whose slope provides E_a calculation. This method is known as Flynn–Wall–Ozawa (FWO) method.

In the Kissinger–Akahira–Sunose (KAS) method [22,23], the expression $p(x)$ is expressed using the Coats–Redfern

approximation [24]:

$$p(x) \cong \frac{\exp(-x)}{x^2} \tag{9}$$

Substituting this into Eq. (6) and taking logarithms we obtain

$$\ln\left(\frac{\beta}{T^2}\right) \cong \ln\left[\frac{AR}{g(\alpha)E_a}\right] - \frac{E_a}{RT} \tag{10}$$

A plot of $\ln(\beta/T^2)$ versus $1/T$ for a constant conversion gives the E_a at that conversion.

The composite methods presuppose one single set of the kinetic parameters for all conversions and heating rates. In this way all the experimental data can be superimposed in one single master curve. Composite differential method I [25] is based directly on Eq. (1) and can be presented in the following form:

$$\ln\left[\frac{\beta\left(\frac{d\alpha}{dT}\right)}{f(\alpha)}\right] = \ln A - \frac{E_a}{RT} \tag{11}$$

For each form of $f(\alpha)$, the curve $\ln[\beta(d\alpha/dT)/f(\alpha)]$ versus $1/T$ was plotted for the experimental data obtained at the different heating rates. We then chose the kinetic model for which the data falls in a single master straight line and which gives the best linear correlation coefficient. A single set of kinetic parameters, E_a and A, can be obtained from the slope and the intercept of the straight line.

3.1. Kinetic model determination

Once the apparent activation energy has been determined, it is possible to search for the most suitable kinetic model for the investigated process. Two special functions, $y(\alpha)$ and $z(\alpha)$, which can easily be obtained by a simple transformation of thermo-analytical data, are defined for this purpose. In non-isothermal conditions these functions can be formulated as follows [26,27]:

$$y(\alpha) = \left(\frac{d\alpha}{dt}\right)\exp(x) \tag{12}$$

$$z(\alpha) = \pi(x)\left(\frac{d\alpha}{dt}\right)\left(\frac{T}{\beta}\right) \tag{13}$$

where $x = E_a/RT$, $\pi(x)$ is an approximation of the temperature integral. The Senum–Yang fourth rational approximation was used in this work [28]. It has been verified that the shape of the $y(\alpha)$ function, as well as the maximum α_M of the $y(\alpha)$ function and α_P^{∞} of the function $z(\alpha)$, can be used to guide the choice of a kinetic model [26,27,29]. For practical reasons, the $y(\alpha)$ and $z(\alpha)$ functions are normalized within the (0,1) ranges. If there are considerable differences in the shape of the $y(\alpha)$ and $z(\alpha)$ functions then, we can conclude that the assumption in which the kinetic model was considered to be a single-step model has not fulfilled.

4. Results and discussion

The experimental non-isothermal conversion (α–T) curves for decomposition process of anhydrous nickel nitrate under air atmosphere at the different heating rates ($\beta = 5$, 15 and 30 K min^{-1}) are shown in Fig. 2.

Fig. 2 shows that all conversion curves exhibit a sigmoidal character, and they are shifted to a higher temperature values as far as the heating rate increases.

The corresponding differential conversion curves for the decomposition of anhydrous nickel nitrate in air atmosphere obtained at different heating rates ($\beta = 5$, 15 and 30 K min^{-1}) are shown in Fig. 3.

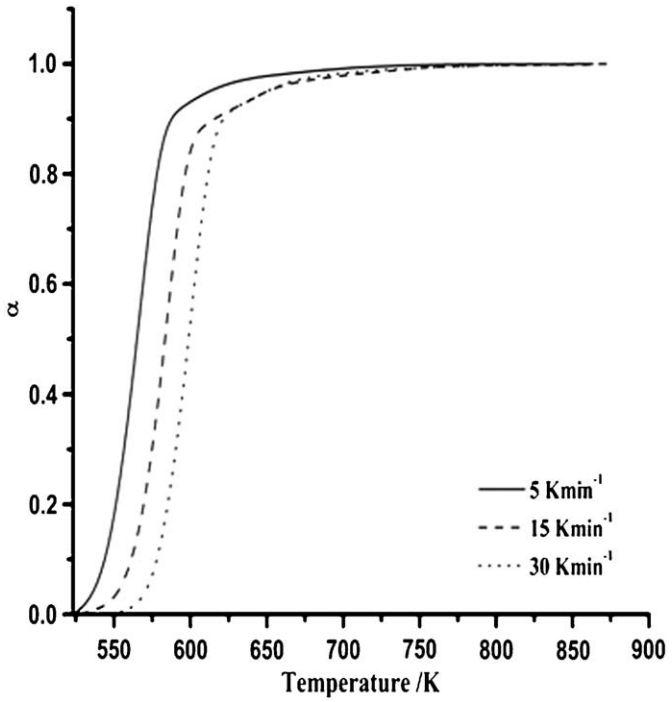

Fig. 2. The experimental conversion (α–T) curves for the non-isothermal decomposition of the anhydrous nickel nitrate in air atmosphere at $\beta = 5$, 15 and 30 K min^{-1}.

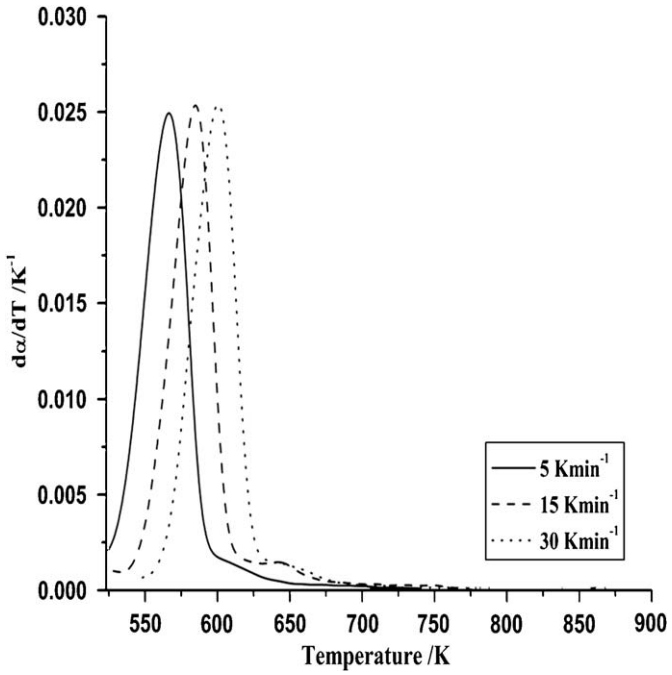

Fig. 3. The experimental differential conversion ($d\alpha/dT$ versus T) curves obtained from the integral conversion curves, for the non-isothermal decomposition of anhydrous nickel nitrate in air atmosphere at $\beta = 5$, 15 and 30 K min^{-1}.

It can be observed that with increase in heating rate (β), the rate of decomposition process shows increasing behavior (Fig. 3).

Fig. 4 shows E_a values as a function of conversion fraction α, determined by FR, FWO and KAS isoconversional methods, for the investigated decomposition process.

As we know, if the determined apparent activation energies are the same for the various values of α, a single-step reaction is

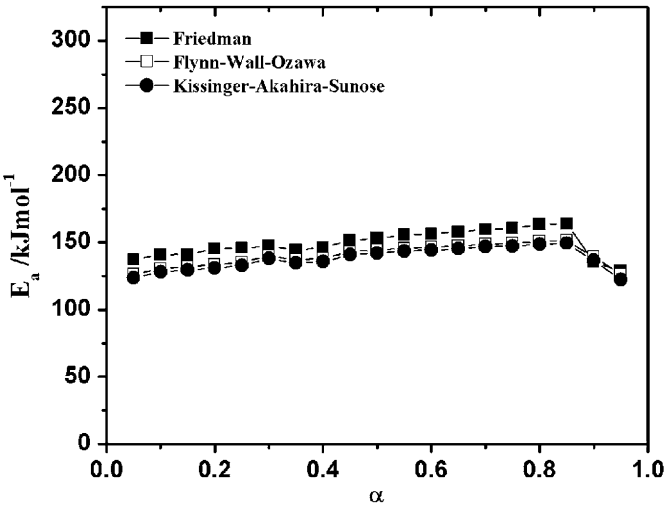

Fig. 4. Dependency of the apparent activation energy (E_a) on the conversion fraction (α) calculated using the Friedman (FR), Flynn–Wall–Ozawa (FWO) and Kissinger–Akahira–Sunose (KAS) isoconversional (model-free) methods from the TG data, for the decomposition process of anhydrous nickel nitrate in air atmosphere.

certainly concluded. On the contrary, a variable E_a with increasing of conversion fraction is an indication of a complex reaction, which will be more serious if the total reaction involves the competitive reactions. Applying the average value of E_a within α of 0.20–0.80 rather than the entire range was strongly recommended because most reactions, especially solid-state ones, are not stable at the beginning and ending periods. Different from solution reaction, solid-state reaction usually contains a diffusion process, the well-known mass and heat-transfer phenomenon [30,31] at the beginning period. It generates temperature and partial pressure gradient. Consequently, it generates reaction gradient from the outer to the inner surface of the solid sample. This phenomenon is almost unavoidable even under strict sample size control (<1 mm). As a result, the real activation energy values at this period are different from the ones at the middle period (0.1 or 0.2 to around 0.8). Thus, using the apparent activation energy E_a to calculate the reaction model parameters in this period will result in some discrepancies. Bearing in mind these facts, we are found the following verage values of E_a in the conversion range of $0.20 \leqslant \alpha \leqslant 0.80$: $E_{a,FR} = 152.8\,\mathrm{kJ\,mol^{-1}}$ (FR), $E_{a,FWO} = 143.1\,\mathrm{kJ\,mol^{-1}}$ (FWO) and $E_{a,KAS} = 140.9\,\mathrm{kJ\,mol^{-1}}$ (KAS), respectively.

It can be pointed out that E_a values determined by means of integral isoconversional methods ($E_{a,FWO}$ and $E_{a,KAS}$) are in a good mutual agreement, while these determined by Friedman differential method ($E_{a,FR}$) are slightly higher ($\Delta E_a = 11.9\,\mathrm{kJ\,mol^{-1}}$).

Differences between $E_{a,FR}$ and E_a calculated by different integral isoconversional methods may be attributed to different ways to derive the relations being the background of these methods. These relations are derived considering that the kinetic parameters do not depend on the conversion fraction. Obviously, if E_a and A depends on the conversion fraction (α), these derivations are not correct. Therefore, in such cases, the Friedman (FR) method, which uses directly the equation of reaction rate, is recommended [32]. The susceptibility of the Friedman (FR) method to errors arising from experimental noise can be effectively mitigated if the rate of data recording during experiments is high so that the raw data can be significantly smoothed prior to the application of the derivative-based Friedman technique. So with proper smoothing of the data, the Friedman technique seems to be a reliable technique in all cases. Among the two integral isoconversional methods used in this work, the kinetic measurements and predictions from the KAS method seem to be much more accurate than the FWO method (which includes a very crude approximation of the temperature integral $p(x)$ in Eq. (6)), but less accurate than the derivative-based Friedman (FR) method.

For determination of kinetic model of the investigated process, the two special functions $y(\alpha)$ and $z(\alpha)$ given by Málek [26,27] have been involved in the consideration. Fig. 5 shows the plots of $y(\alpha)$ and $z(\alpha)$ functions as a function of conversion fraction, α.

The values of both $y(\alpha)$ and $z(\alpha)$ were normalized within the (0,1) interval. It is clear that the shapes of the $y(\alpha)$ and $z(\alpha)$ plots, are practically invariant with respect to the heating rate. The values of α_M and α_P^{∞} corresponding to the maxima of the $y(\alpha)$ and $z(\alpha)$ functions are summarized in Table 1.

The values fall into the ranges $0.15 \leqslant \alpha_M \leqslant 0.18$ and $0.49 \leqslant \alpha_P^{\infty} \leqslant 0.61$, respectively. These variances correspond to the variances in the calculated values of the apparent activation energies (for the construction of $y(\alpha)$ and $z(\alpha)$ functions, the apparent activation energy (E_a) calculated from Friedman's isoconversional method was used).

The value of α_M show that the kinetic data can be described by Johnson–Mehl–Avrami (JMA) ($n>1$) [33–36] and/or Šesták–Berggren (SB(M, N)) model [37]. But the α_P^{∞} value is far lower than the value predicted for JMA model ($\alpha_P^{\infty} = 0.63$), it seems that one or more conditions for the applicability of the JMA model is not fulfilled for the decomposition process of anhydrous nickel nitrate.

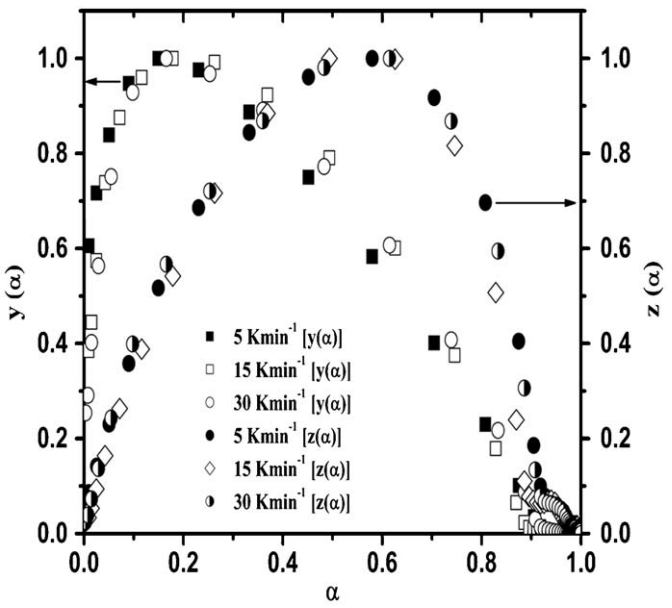

Fig. 5. The normalized $y(\alpha)$ and $z(\alpha)$ functions of decomposition process of anhydrous nickel nitrate in air atmosphere, obtained from the non-isothermal TG data at three different heating rates ($\beta = 5$, 15 and $30\,\mathrm{K\,min^{-1}}$).

Table 1
The maximum of the $y(\alpha)$ function α_M and $z(\alpha)$ function α_P^{∞} evaluated for the non-isothermal decomposition process of anhydrous nickel nitrate under air atmosphere.

β ($\mathrm{K\,min^{-1}}$)	α_M	α_P^{∞}
5	0.15	0.58
15	0.18	0.49
30	0.17	0.61

Recently, it was reported [38,39] that the traditional kinetics model functions $f(\alpha)$ of solid-state reactions are not appropriate to describe the real process, which requires take account of shape irregularity, shielding and overlapping, unequal mixing anisotropy and so on, for the particles formed during reaction. In this case, it would be useful to find an empirical function $f(\alpha)$ containing the smallest number of constants as far as possible, giving a flexibility sufficient to describe the real thermoanalytical data. That the empirical kinetics function was proposed by Šesták and Berggren [37], in the form:

$$f(\alpha) = \alpha^M(1-\alpha)^N \tag{14}$$

which is usually named as SB(M, N) kinetic model. The parameters M and N are the relative contributions of acceleratory and decay regions of the considered kinetic process and they are also taken as kinetic parameters describing the shape of measured thermoanalytical curve. The SB kinetic model can be used for a quantitative description of more complex crystallization processes involving partially overlapping nucleation and growth phases. The kinetic exponents, M and N in Eq. (14), are characteristic of a particular crystallization process although it is rather problematic to find their real physical meanings. It was shown [40], however, that the physically meaningful values of the parameter M (in Eq. (14)) should be confined in the range of $0<M<1$.

As mentioned above, the investigated process do not show a simple crystallization kinetics as expressed by JMA model and the value of α_P^{∞} which is far lower than 0.63. Such a behavior is perhaps a consequence of the fast increase of the initial crystallization rate. This acceleration can be due to a secondary nucleation induced by the crystal growth. Such behavior can be described by means of the empirical two-parameter SB(M, N) reaction model, which is applicable in the field of crystallization kinetics according to the discussion given above and the diagram proposed by Málek [26].

For SB(M, N) model, the kinetic parameter ratio is calculated using the following expression [26]:

$$P = \frac{M}{N} = \frac{\alpha_M}{(1-\alpha_M)} \tag{15}$$

and N can be obtained by the following formula [26]:

$$\ln\left[\left(\frac{d\alpha}{dt}\right)\exp\left(\frac{E_a}{RT}\right)\right] = \ln A + N\ln[\alpha^p(1-\alpha)] \tag{16}$$

That is, the kinetic parameter N corresponds to the slope of the linear plot of $\ln[(d\alpha/dt)\exp(E_a/RT)]$ versus $\ln[\alpha^P(1-\alpha)]$ when $0.20\leqslant\alpha\leqslant0.80$. Then, the second kinetic parameter M is $M = PN$.

Because of its widespread availability to an easy-to-use data analysis software form, the SB equation is often to model crystallization process with surprisingly good fit.

Using formulae (15)–(16), the kinetic parameters in SB(M, N) kinetic model for the investigated decomposition process are calculated and shown in Table 2.

It can be observed from Table 2 that the SB kinetic exponent (M) varies in the range of $0.21\leqslant M\leqslant0.26$. On the other hand, the SB kinetic exponent N decreases with the increase in the heating rate. Taking these values (Table 2) we calculated average kinetic parameters for the SB(M, N) reaction model as follows: $M = 0.23$, $N = 1.14$ and $A = 1.10\times10^{13}\,\mathrm{min}^{-1}$.

According to Eqs. (1) and (14), the theoretical (SB kinetic model) (symbols) and experimental (lines) differential rate curves at heating rates of $\beta = 5$, 15 and 30 K min^{-1} were calculated and presented in Fig. 6.

As observed, the theoretical curves calculated from SB model are very close to the experimental differential rate curves (Fig. 6) with very good fitting ($R^2>0.9985$). So, one may expect that the SB model obtained from $y(\alpha)$ and $z(\alpha)$ functions is suitable to describe the decomposition process of anhydrous nickel nitrate.

To provide a complete kinetic view, the reliability of $\ln A$ was also checked using an alternative method based on the second derivative of α (second-derivative method [26], Eq. (17)). The pre-exponential factor A (Eq. (17)) may be obtained for every mechanism from the derivative of $f(\alpha)$, $f'(\alpha)$, assuming the validity of $f(\alpha)$ [26]

$$A = -\frac{\beta(x_p)}{f'(\alpha_p)T_p}\exp(x_p) \tag{17}$$

where β is the heating rate, $x_p = E_a/RT_p$, T_p the peak temperature on the differential conversion curve and α_p is the conversion value which corresponds to the peak temperature T_p.

The application of the above-described method is illustrated in the present paper for the non-isothermal decomposition process of anhydrous nickel nitrate. The values of peak temperature (T_p), derivative ($f'(\alpha)$) and the pre-exponential factor (A) calculated by applying Eq. (17) at different heating rates (β) are shown in Table 3.

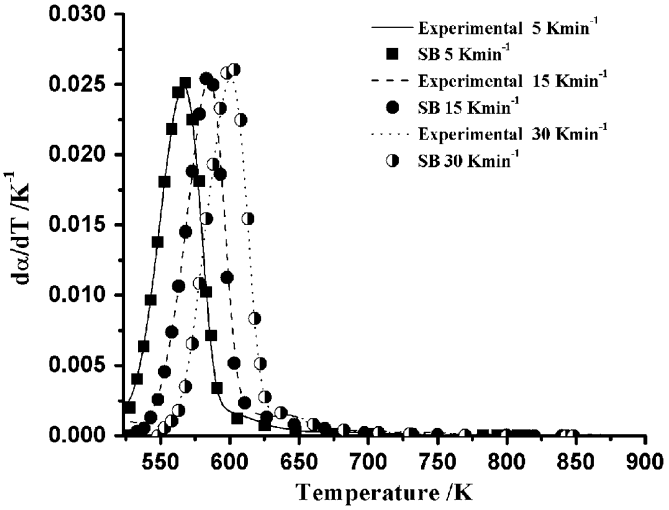

Fig. 6. Comparison of the experimental and calculated differential conversion curves using the SB(M,N) kinetic model (Table 2) at three different heating rates ($\beta = 5$, 15 and 30 K min^{-1}).

Table 2
Kinetic parameters from the SB kinetic model evaluated for the investigated decomposition process of anhydrous nickel nitrate at the different heating rates.

β (K min^{-1})	SB kinetic model			
	P (M/N)	M	N	$\ln A$ (A min^{-1})
5	0.18	0.22	1.23	30.03
15	0.22	0.26	1.16	30.13
30	0.20	0.21	1.03	29.93
Average	0.20	0.23	1.14	30.03

Table 3
Determination of the pre-exponential factor (A) for decomposition process of anhydrous nickel nitrate at the different heating rates using the second-derivative method (Eq. (17)).

β (K min^{-1})	T_p (K)	f' (α_p)	A ($\times10^{13}$ min^{-1})
5	568.16	−0.76860	4.14
15	583.16	−0.65751	6.00
30	603.16	−0.78165	3.32

Table 3 shows that the value of peak temperature (T_p) increases with increasing in heating rate (β), which is typical for the thermally activated heterogeneous process. On the other hand, the values of the pre-exponential factor (A) at all heating rates (Table 3, column 4) are in good agreement with average value of A calculated using Eq. (16) ($1.10\times10^{13}\,\mathrm{min}^{-1}$) (in the respect to the order of A ($\times10^{13}$)).

In order to check the established reaction model, we are applied the composite differential method I [25] (Eq. (11)).

Fig. 7 shows how all the data for the SB differential conversion function $f(\alpha)=\alpha^{0.23}(1-\alpha)^{1.14}$ fits onto just one master straight line.

It can be seen from Fig. 7 that all points are placed around/on the same line only for the SB kinetic exponents $M=0.23$ and $N=1.14$. From the parameters of this straight line the Arrhenius parameters were evaluated, and the corresponding values are: $E_a=147.1\,\mathrm{kJ\,mol}^{-1}$, $\ln A=30.19$ (A in min^{-1}), where adj. R-square $R^2=0.9928$. The obtained value of E_a is the medium value between the values of the apparent activation energy calculated by FR method ($E_{a,FR}=152.8\,\mathrm{kJ\,mol}^{-1}$) and FWO method ($E_{a,FWO}=143.1\,\mathrm{kJ\,mol}^{-1}$).

If we chosen the appropriate kinetic model, the relative deviation (e%) of the apparent activation energy (E_a) calculated by composite differential method I, in respect to the value of E_a obtained by isoconversional method, does not exceed 10% in absolute value. This statement can be presented by the following equation [41–43]:

$$e\% = \frac{E_a(iso)-E_a(SB)_{comp.}}{E_a(iso)}\times 100 \qquad (18)$$

where $E_a(iso)$ and $E_a(SB)_{Comp}$. represents the apparent activation energy value calculated by isoconversional and composite differential method I, respectively.

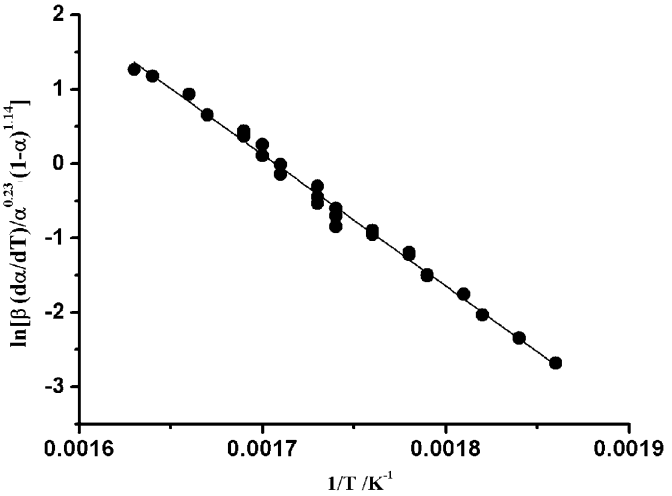

Fig. 7. Composite differential method analysis of the non-isothermal TG data (5, 15 and 30 K min^{-1}) based on Eq. (11) for decomposition process of anhydrous nickel nitrate in air atmosphere. The full circles correspond to the differential data, for the SB(M,N) kinetic model with exponents $M=0.23$ and $N=1.14$.

Table 4
The relative deviation (e %) values calculated from Eq. (18) for considered isoconversional kinetic methods.

Isoconversional method	e (%)
Friedman	3.73
Kissinger–Akahira–Sunose	−4.40
Flynn–Wall–Ozawa	−2.79

Table 4 shows the values of e (in %) calculated for the apparent activation energy values estimated from three different isoconversional methods (FR, KAS and FWO).

Based on the established values of e (Table 4), we can confirmed that in the investigated conversion range, the decomposition process follow the two-parameter autocatalytic SB(M, N) reaction mechanism.

Based on these results, we may conclude that if the maximum of $z(\alpha)$ function is shifted to lower values of conversion fraction ($\alpha_P^{\infty}<0.63$) the conditions of validity of the JMA model are not fulfilled. Such a displacement indicates increasing complexity of the process and can be caused by the influence of surface nucleation. Nevertheless, the complex behavior can also be observed when the temperature distribution within the sample is affected considerably by liberation of the heat of crystallization [44]. In addition, if the maximum of the $y(\alpha)$ function is shifted to higher values of α, it clearly indicates an increasing influence of the product (crystallized phase) to the overall crystallization kinetics [45]. This behavior is characteristic for autocatalytic reaction systems which can be best described by the Šesták–Berggren (SB) model.

The increasing value of the kinetic exponent M indicates a more important role of the crystallized phase on the overall kinetics. For non-isothermal decomposition of anhydrous nickel dinitrate under air atmosphere, the exponent M catch the maximal value at the medial value of heating rate (15 K min^{-1}) (Table 2). On the other hand, the higher value of the kinetic exponent $N>1$ means the increasing complexity (Table 2).

From Table 2 it can be observed that with increasing of heating rate, the value of kinetic exponent N decreasing, which causes the reduction of complexity of the investigated process. However, the global influence of heating rate on M, N and $\ln A$ values (Table 2) is very small and can be neglected.

It can be observed from Fig. 4 that after conversion value of $\alpha=0.85$, the apparent activation energy of decomposition process decreases for about $35\,\mathrm{kJ\,mol}^{-1}$ from the initial value in the mentioned point. This decrease of E_a value at the end of the investigated process may be caused by an additional autocatalytic effect of NO_2, which depends on the gas partial pressure directly linked with concentration of evolved gas. In addition, it can be pointed out that the products of the low pressure CRTA (Constant Rate Thermal Analysis) thermolysis of nickel nitrate hexahydrate are characterised by remarkably high surface areas ($80\,\mathrm{m}^2\,\mathrm{g}^{-1}$ for nickel oxide) while apparently the same reaction carried out under higher pressures gives products with an undeveloped surface [46]. On the other hand, the anhydrous nickel nitrate has the much lower specific surface area ($18\,\mathrm{m}^2\,\mathrm{g}^{-1}$) [46]. Accordingly, the heating of the anhydrous nickel nitrate in the temperature range of $525\,\mathrm{K}\leqslant T\leqslant 875\,\mathrm{K}$, probably leads to both an increase in the specific surface area and decrease in grain size of the catalyst. In accordance with Málek's theory [47] such behavior clearly indicates a more complex crystallization mechanism. The coarse powder sample exhibit a slightly higher value of α_P^{∞}, but it is still below the value typical for the JMA kinetic model.

The empirical SB(M,N) kinetic model accommodates the discrepancy of the real process from the idealized process, with the flexibility enough to describe the real decomposition process as closely as possible. It can be concluded that the $z(\alpha)$ function for decomposition process of anhydrous nickel nitrate under air atmosphere clearly shows the position of maximum lower than 0.63 ($\alpha_P^{\infty}<0.63$), and in that case one (or more) of the aforementioned conditions is not fulfilled and the JMA model cannot not be used for description of the experimental data. Usually, it is because of overlapping of nucleation and crystal growth processes with the result that the site saturation condition is no longer held. Therefore, the SB kinetic model can be used for a

quantitative description of non-isothermal decomposition process of anhydrous nickel nitrate which involves the partially overlapping nucleation and growth phases.

5. Conclusions

Kinetic analysis of non-isothermal decomposition process of anhydrous nickel nitrate in air atmosphere was performed using three different isoconversional (model-free) methods. For determination of kinetic model function of considered process, the Málek's method was used. The composite differential method I was used for checking the established reaction model. It was found that the value of E_a calculated by composite differential method ($E_a = 147.1\ \mathrm{kJ\,mol^{-1}}$) represents the medium value between the values of the apparent activation energy calculated by FR ($E_{a,FR} = 152.8\ \mathrm{kJ\,mol^{-1}}$) and FWO ($E_{a,FWO} = 143.1\ \mathrm{kJ\,mol^{-1}}$) isoconversional methods.

It was found that the two-parameter autocatalytic model (Šesták–Berggren (SB) equation) with kinetic exponents $M = 0.23$ and $N = 1.14$ is the most adequate one to describe the decomposition kinetics of the studied system at various heating rates. The obtained non-isothermal differential conversion curves from the experimental data show the results being accordant with those theoretically calculated.

It was established that the evaluated Šesták–Berggren (SB) kinetic model can be used for a quantitative description of the non-isothermal decomposition process of anhydrous nickel nitrate which involves the partially overlapping nucleation and growth phases.

Acknowledgments

This study was partially supported by the Ministry of Science and Environmental Protection of Serbia, under the following Projects 142025 and 142047 (S. Mentus).

References

[1] European Nickel Group, Speciality Inorganic Chemicals BREF (BAT (best available techniques) reference document) Note-Soluble Inorganic Salts of Nickel—General Information—Final Draft, Rev. 2, March 2004, 2004.
[2] European Nickel Group, SIC (speciality inorganic chemicals) BREF Notes—Inorganic Soluble Nickel Salts—Data from the producers, 2004.
[3] European IPPC (integrated pollution prevention and control) Bureau, Reference Document on Best Available Techniques in the Non Ferrous Metals Industries, 2001.
[4] European IPPC (integrated pollution prevention and control) Bureau, Draft Reference Document on Best Available Techniques for the Production of Large Volume Inorganic Chemicals (Ammonia, Acids and Fertilisers), 2004.
[5] P. Thomasson, O.S. Tyagi, H. Knözinger, Appl. Catal. A Gen. 181 (1999) 181–188.
[6] E. Ruckenstein, Y.H. Hu, Appl. Catal. A Gen. 183 (1999) 85–92.
[7] A. Parmaliana, F. Arena, F. Frusteri, S. Coluccia, L. Marchese, G. Martra, A.L. Chuvilin, J. Catal. 141 (1993) 34–47.
[8] W. Brockner, C. Ehrhardt, M. Gjikaj, Thermochim. Acta 456 (2007) 64–68.
[9] J.M. Criado, A. Ortega, C. Real, React. Solids 4 (1987) 93–103.
[10] L.A. Pérez-Maqueda, A. Ortega, J.M. Criado, Thermochim. Acta 277 (1996) 165–173.
[11] J.M. Criado, L.A. Pérez-Maqueda, J. Therm. Anal. Calorim. 80 (2005) 27–33.
[12] J.M. Criado, L.A. Pérez-Maqueda, SCTA and kinetics, in: O.T. Sørensen, J. Rouquerol (Eds.), Sample Controlled Thermal Analysis, Kluwer, Dordrecht, Holland, 2003, pp. 62–101.
[13] F.J. Gotor, L.A. Pérez-Maqueda, A. Ortega, J.M. Criado, J. Therm. Anal. Calorim. 53 (1998) 389–396.
[14] T. McAllister, J. Anal. Atomic Spectrom. 9 (1994) 427–430.
[15] H.L. Friedman, J. Polym. Sci. C 6 (1963) 183–195.
[16] M.E. Brown, Introduction to Thermal Analysis: Techniques and Applications, second ed., Kluwer, Amsterdam, 2001 (Chapter 10).
[17] A.K. Galwey, M.E. Brown, Thermal Decomposition of Ionic Solids: Chemical Properties and Reactivities of Ionic Crystalline Phases, Elsevier, Amsterdam, 1999, pp. 139–171.
[18] W. Gautschi, W.F. Cahill, Exponential integral and related functions, in: M. Abramowitz, I. Stegun (Eds.), Handbook of Mathematical Functions with Formulas Graphs and Mathematical Tables, National Bureau of Standards, Washington, DC, 1964, pp. 227–237.
[19] H.J. Flynn, L.A. Wall, J. Res. Natl. Bur. Stand. A Phys. Chem. 70 (1966) 487–523.
[20] T. Ozawa, Bull. Chem. Soc. Jpn. 38 (1965) 1881–1886.
[21] C.D. Doyle, J. Appl. Polym. Sci. 5 (1961) 285–292.
[22] H.E. Kissinger, Anal. Chem. 29 (1957) 1702–1706.
[23] T. Akahira, T. Sunose, Res. Rep. Chiba Inst. Techn. 16 (1971) 22–31.
[24] A.W. Coats, J.P. Redfern, Nature 201 (1964) 68–69.
[25] J.M. Criado, L.A. Pérez-Maqueda, F.J. Gotor, J. Málek, N. Koga, J. Therm. Anal. Calorim. 72 (2003) 901–906.
[26] J. Málek, Thermochim. Acta 200 (1992) 257–269.
[27] J. Málek, Thermochim. Acta 138 (1989) 337–346.
[28] G.I. Senum, R.T. Yang, J. Therm. Anal. Calorim. 11 (1977) 445–447.
[29] M.E. Brown, D. Dollimore, A.K. Galwey, Reactions in the Solid State, Elsevier, Amsterdam, 1982, pp. 41–113.
[30] N. Koga, J.M. Criado, Int. J. Chem. Kinet. 30 (1998) 737–744.
[31] N. Koga, J.M. Criado, J. Am. Ceram. Soc. 81 (1998) 2901–2909.
[32] P. Budrugeac, E. Segal, Int. J. Chem. Kinet. 33 (2001) 564–573.
[33] W.A. Johnson, R.T. Mehl, Trans. AIME 135 (1939) 416–458.
[34] M. Avrami, J. Chem. Phys. 7 (1939) 1103–1112.
[35] M. Avrami, J. Chem. Phys. 8 (1940) 212–224.
[36] M. Avrami, J. Chem. Phys. 9 (1941) 177–184.
[37] J. Šesták, G. Berggren, Thermochim. Acta 3 (1971) 1–12.
[38] N. Koga, J. Šesták, J. Málek, Thermochim. Acta 188 (1991) 333–336.
[39] N. Koga, J. Šesták, J. Therm. Anal. Calorim. 37 (1991) 1103–1108.
[40] J. Málek, J.M. Criado, J. Šesták, J. Militký, Thermochim. Acta 153 (1989) 429–432.
[41] P. Budrugeac, E. Segal, J. Therm. Anal. Calorim. 82 (2005) 677–680.
[42] E-H.M. Diefallah, M.A. Gabal, A.A. El-Bellihi, N.A. Eissa, Thermochim. Acta 376 (2001) 43–50.
[43] E-H.M. Diefallah, S.N. Basahl, A.Y. Obaid, R.H. Abu-Eittah, Thermochim. Acta 111 (1987) 49–56.
[44] D.W. Henderson, J. Non-Cryst. Solids 30 (1979) 301–315.
[45] J. Málek, E. Černošková, R. Švejka, J. Šesták, G. Van der Plaats, Thermochim. Acta 280–281 (1996) 353–361.
[46] E.A. Fesenko, P.A. Barnes, G.M.B. Parkes, Sample controlled thermal analysis, in: O.T. Sørensen, J. Rouquerol (Eds.), Origin Goals Multiple Forms Applications and Future, Springer, Berlin, 2003, pp. 182–183.
[47] J. Málek, Thermochim. Acta 355 (2000) 239–253.